Science and Technology Indonesia
e-ISSN:2580-4391 *p*-ISSN:2580-4405
Vol. 6, No. 4, October 2021

Research Paper

Application of Non-Linear Kinetic and Isotherm Model for Investigation of Cod Removal from Tapioca Liquid Waste Onto Modified Lampung Natural Zeolite

Didik Supriyadi[1]*, Darmansyah[2], Ratna Puspita Sari[2], Amna Citra Farhani[3]

[1]*Department of Chemical Engineering, Institut Teknologi Sumatera, Lampung Selatan, 35365, Indonesia*
[2]*Department of Chemical Engineering, University of Lampung, Bandar Lampung, 35365, Indonesia*
[3]*Department of Biosystems Engineering, Institut Teknologi Sumatera, Lampung Selatan, 35365, Indonesia*
***Corresponding author**: didik.supriyadi@tk.itera.ac.id

Abstract
The experimental data analysis of tapioca liquid waste onto modified Lampung natural zeolite using non-linear regression models is limited. The adsorption data were analyzed with nine kinetic models (the pseudo-first-order, the pseudo-second-order, the intraparticle diffusion, fractional power, Bangham, Elovich, mixed-1.2-order, modification of pseudo-second-order, and Avrami) and eight isotherm models (Langmuir, Freundlich, Dubinin-Radushkevich, Sips, Redlich-Peterson, Toth, Liu, and Khan). The percentage of adsorption was decreased from 61.29% to 13.66% with increasing Chemical Oxygen Demand (COD) concentration 310 mg/L to 9450 mg/L. The result showed that the power model (R^2: 0.98, X^2: 0.137), Avrami (R^2: 0.98, X^2: 0.141), Bangham (R^2: 0.98, X^2: 0.145) and modified pseudo-second-order (R^2: 0.98, X^2: 0.147) can be recommended as the best fitted to experimental kinetic data. The Khan model (R^2: 0.99961, X^2: 0.03729) and Langmuir (R^2: 0.99478, X^2: 0.24902) was the most reliable for describing the isotherm model. Thus, the analysis of experimental adsorption data using a non-linear regression model is highly recommended.

Keywords
Adsorption, Fractional-power, Khan-model, Non-linear, Tapioca Liquid Waste

Received: 20 April 2021, Accepted: 08 July 2021
https://doi.org/10.26554/sti.2021.6.4.218-227

1. INTRODUCTION

Indonesia, the world's fourth-largest cassava producer, will face environmental issues related to liquid waste from cassava industries, such as odorous smell in the river and underground water resource pollution (Hermiati et al., 2012). These environmental issues will occur if liquid wastes are not handled correctly. It is caused the cassava liquid waste contains high chemical oxygen demand (COD), biochemical oxygen demand (BOD), and total solids content (TS) (Edama et al., 2014). Several treatments have been applied for reducing COD, such as the precipitation process, microbiology process, chemical reaction, and adsorption process. The adsorption process is cheaper, easy to operate, and high efficiency when compared with the other method (de la Luz-Asunción et al., 2019). The quality of the adsorbent will determine the performance of the adsorption process (Mohadi et al., 2017). The widely used adsorbent material for the adsorption process is zeolite (Wang and Peng, 2010). Zeolites are three-dimensional aluminosilicate and have been used successfully as an effective adsorbent for removing water contaminants (Liu et al., 2017). Zeolite must be modified with cationic surfactants for improving its adsorptive capacity towards organic pollutants. The addition of cationic surfactants such as cetyltrimethylammonium bromide (CTAB) has shown increasing organic compounds' absorption ability. A previous study revealed that modified graphite with CTAB had excellent adsorption capacity for bisphenol A (BPA) (Wang et al., 2018). The other study showed the modification of chitosan with CTAB increased its ability to adsorb dye from wastewater (Guo et al., 2012).

Many researchers have conducted studies about removing COD through the adsorption process from wastewater. The study about COD removal from purified terephthalic acid (PTA) using granular activated carbon (GAC) showed that COD adsorption followed the pseudo-second-order kinetic model (Verma et al., 2014). The other experiment showed that powdered activated coke had a higher COD removal than other activated carbon, and the equilibrium time was reached in 20 minutes (Shen et al., 2019). The investigation of ammonia and COD adsorption using different adsorbents (zeolite, activated carbon, and composite) has been conducted (Halim et al., 2010). The result of the study showed all adsorbents were fitted with Langmuir and Freundlich

isotherm (R^2 > 0.9) for ammonia adsorption. For COD adsorption, both zeolite and composite material followed the pseudo-second-order kinetic model. In contrast, activated carbon obeyed the pseudo-first-order and intra-particle. Removal of COD using coal fly ash has been reported. The adsorptive capacity of COD from tapioca waste was 15.92 mg/g, and equilibrium data were fitted with The Langmuir isotherm model (Darmansyah et al., 2016). The use of activated bagasse fly ash to adsorb distillery spent wash has been investigated. When the initial COD concentration was increased from 1000 mg/L to 6000 mg/L, the adsorption capacity increased from 6 to 92.40 mg/L, and the removal efficiency increased from 24 to 61.6% (Fito et al., 2017).

Many studies often used the linearized kinetic and isotherm model for predicting adsorption parameters. However, previous studies showed that fitting experimental kinetic and isotherm data with calculation data was better with the non-linear model than the linear model (Moussout et al., 2018; Kumar et al., 2008). The studies about comparison linear and non-linear models have been investigated and reported. The result showed that adsorption Cd(II) and Zn(II) on macrofungus obeyed sips non-linear isotherm model and non-linear pseudo-second-order kinetic model (Nagy et al., 2017). The other study revealed that non-linear kinetic and isotherm models were better to determine adsorption parameters. This study also showed the Langmuir isotherm model and the pseudo-second-order model fitted well better than other models (de la Luz-Asunción et al., 2019).

In this study, experimental data of COD adsorption are examined with nine non-linear kinetic models: the pseudo-first-order, the pseudo-second-order, the intraparticle diffusion, fractional power, and Bangham, Elovich mixed-1.2-order, modification of pseudo-second-order, and Avrami. The eight isotherm models used the Langmuir, Freundlich, Dubinin-Radushkevich, Sips, Redlich-Peterson, Toth, and Khan were also fitted with experimental isotherm data. The five different error functions were used to evaluate the parameter of kinetic and isotherm models by minimizing the error function.

2. EXPERIMENTAL SECTION

2.1 Zeolite Modification with CTAB

Before modifying zeolite with the CTAB, zeolite was activated with 20 mL NH_4Cl 1.5 M. Zeolite with NH_4Cl solution was stirred at 350 rpm for 12 hours. After washing and filtering, zeolite was calcined at 350°C for 9 hours. A 7 grams calcined zeolite was reacted with 100 mL of CTAB with a concentration of 100 mM. The mixture was stirred at 150 rpm for 24 hours. After stirring, the mixture was filtered and washed with distilled water to neutral pH. The neutral zeolite was dried at 70°C for 5 hours (Darmansyah et al., 2021).

2.2 Characterization of Zeolite

The modified zeolites were characterized by Fourier transmission infrared (FTIR), Scanning electron microscope (SEM), X-ray diffraction (XRD), Brunauer–Emmett–Teller (BET) (Darmansyah et al., 2021).

2.3 Adsorption Experiment

To collecting data for the optimization modeling data Lampung natural zeolite was modified with CTAB 100mM. One gram of modified adsorbent was contacted with 100 mL tapioca liquid waste at different COD initial concentrations (310 mg/L-9450 mg/L). The residual COD was measured by spectrophotometric.

$$q_e = \frac{(C_0 - C_e)\text{x V}}{\text{W}} \quad (1)$$

Where C_0 and C_e are the initial and the equilibrium concentrations in a liquid phase (mg/L), V is the volume of solution (L), and W is the mass of the adsorbent (g).

2.4 Kinetic and Equilibrium Studies

Kinetic and equilibrium studies were performed by using one gram of adsorbent 100 mL of tapioca liquid waste, and the mixture was stirred at 600 rpm for 2 hours (Darmansyah et al., 2021).

2.5 Error Function

The error function is required for optimizing the fit of the non-linear kinetic and isotherm model. The selection of the error function can influence the obtained parameters of the models. The five error functions were used, such as sum squares of errors (SSE), the sum of the absolute errors (SAE), the average relative error (ARE), the hybrid fractional error (HYBRID), and Marquardt's percent standard deviation (MPSD). The Solver add-in with Microsoft's spreadsheet Excel was used for optimization procedures.

a. The sum of the squares of the errors (SSE)

$$\text{SSE} = \sum_{i=1}^{n} \left(q_{e,calc} - q_{e,exp} \right)_i^2 \quad (2)$$

b. The sum of the absolute errors (SAE)

$$\text{SAE} = \sum_{i=1}^{n} \left| q_{e,calc} - q_{e,exp} \right|_i \quad (3)$$

c. The average relative error (ARE)

$$\text{ARE} = \frac{100}{n} \sum_{i=1}^{n} \left| \frac{q_{e,calc} - q_{e,exp}}{q_{e,exp}} \right|_i \quad (4)$$

d. The hybrid fractional error function (HYBRID)

$$\text{HYBRID} = \frac{100}{n-p} \sum_{i=1}^{n} \left[\frac{(q_{e,calc} - q_{e,exp})^2}{q_{e,calc}} \right]_i \quad (5)$$

e. Marquardt's percent standard deviation (MPSD)

$$\text{MPSD} = 100 \sqrt{\frac{1}{n-p} \sum_{i=1}^{n} \left(\frac{(q_{e,calc} - q_{e,exp})}{q_{e,calc}} \right)_i^2} \quad (6)$$

The application of the five error functions will produce five parameter sets of the model; therefore, it is difficult to find the optimum parameters result from the calculations. To obtain the

Table 1. Non-Linear Kinetic Models

Kinetic model	Equation		Ref.
Pseudo-first-order	$q_t = q_e\ [1 - \exp(-k_{p1}{}^t)]$	(9)	(Ho and McKay, 1998)
Pseudo-second-order	$q_t = \frac{k_{p2} q_e^2 t}{1+k_{p2} q_e t}$	(10)	(Ho and McKay, 1998)
Intraparticle diffusion	$q_t = k_{ip} \sqrt{t + \theta}$	(11)	(Kuo, 2009)
Fractional power	$q_t = k_p t^v p$	(12)	(Khambhaty et al., 2009)
Bangham	$q_t = k_b t^{1/m}$	(13)	(Rodríguez et al., 2009)
Elovich	$q_t = \frac{ln[\alpha\beta t]}{\beta}$	(14)	(Netzahuatl-Muñoz et al., 2015)
Mixed 1.2 order	$q_t = q_e \frac{1-exp(-kt)}{1-f_0 exp(-kt)}$	(15)	(Marczewski, 2010)
Modified pseudo-second-order	$q_t = \frac{k_{fso} q_e^2 t^\alpha}{1+k_{fso} q_e t^\alpha}$	(16)	(Haerifar and Azizian, 2014)
Avrami	$q_t = q_e\ [1 - \exp(-k_{av} t)^{nav}]$	(17)	(Bergmann and Machado, 2015)

optimum parameter values, the procedure of 'sum normalized errors (SNE)' is usually applied. SNE is calculated by dividing the value of each error function from kinetic and isotherm models with the maximum errors for each error function. The parameters set were gained based on the smallest SNE; hence, that would provide the closest fit to the measured data. After obtaining parameter sets based on the minimum SNE procedure, the coefficient of determination (R^2) and the chi-square (X^2) were adopted to decide the best kinetic and isotherm models.

$$R^2 = \frac{\left(q_{e,exp} - \overline{q_{e,calc}}\right)^2}{\sum \left(q_{e,exp} - \overline{q_{e,calc}}\right)^2 + \left(q_{e,exp} - \overline{q_{e,calc}}\right)^2} \quad (7)$$

$$X^2 = \sum_{i=1}^{n} \frac{\left(q_{e,calc} - q_{e,exp}\right)^2}{q_{e,exp}} \quad (8)$$

The best fit of the model is the one with the lowest chi-square value and the highest coefficient of determination value, which is close to unity.

3. RESULTS AND DISCUSSION

3.1 Characterization of Modified Zeolite

The infrared (IR) spectrum of modified zeolite with CTAB showed a spectrum at 2922.2 cm^{-1} and at 2810.4 cm^{-1} that can be attributed to asymmetric and symmetric C-H band of -CH_2 group in CTAB. The peak at 1625.1 cm^{-1} and 1446.2 cm^{-1} corresponded to asymmetric and symmetric N^+-NH_3 groups, respectively (Darmansyah et al., 2021). The FTIR bands of modified zeolite with CTAB are similar to the previous studies (Anas et al., 2020; Taffarel and Rubio, 2010). SEM analysis also indicated that CTAB could attach to the surface of the zeolite. The XRD patterns showed the main peaks at 2θ= 22.3°, 25.89°, 11.05°, 29.87°, 28.0°. These peaks were identical with clinoptilolite and albite. Based on the result of BET surface area, the modified zeolite has a surface area of 10.893 m^2/g. The pore size diameter and the pore size are 0.0472 cc/g and 74.9755 Å (Darmansyah et al., 2021).

3.2 Effect of Contact Time and Initial Concentration COD

The adsorption of COD was evaluated as a function of time to determine when equilibrium condition. In this study, a 10 ml liquid waste solution was mixed with 1 gr of modified natural zeolite. The sample was taken every 10 minutes, and the concentration of COD was measured (Figure 1(a)). The adsorption of the COD rate was high in the first 10 minutes with 16.4% COD removal. The highest COD percentage removal at the beginning of the adsorption because the modified adsorbent had numerous empty sites during this initial stage. The adsorption rate was decreased gradually in 20 minutes until it reached the equilibrium condition in 90 minutes. To verify whether the equilibrium was reached, the experiment was extended until 100 minutes, and the rate of adsorption was steady. This equilibrium condition was achieved because adsorbents' vacant sites are fully filled by adsorbate (Rodríguez et al., 2009; Verma et al., 2014). The other study had a similar situation that the highest rate of adsorption occurred at the initial time of the adsorption process (Siregar et al., 2021).

Figure 1(b) shows the effect of the initial concentration on the adsorption. In this study, the initial concentration of COD was varied from 310 mg/L to 9450 mg/L. The removal efficiency of COD adsorption at 90 minutes decreased from 61.29% to 13.66% because COD concentration increased from 310 mg/L to 9450 mg/L. Zhao et al., 2013 reported a similar trend that the removal

Table 2. Non-Linear Isotherm Models

Isotherm model	Equation		Ref.
Langmuir	$q_e = \frac{K_L q_{maks} C_e}{1+K_L C_e}$	(18)	(Bergmann and Machado, 2015)
Freundlich	$q_e = K_f C_e^{1/n}$	(19)	(Bergmann and Machado, 2015)
Dubinin-Radushkevich	$q_e = q_s.\exp(-k_{ad}{}^{\varepsilon 2})$	(20)	(Dada, 2012)
Sips	$q_e = \frac{q_{maks} K_R C_e^{\beta_S}}{1+K_R C_e^{\beta_S}}$	(21)	(Bergmann and Machado, 2015)
Redlich-Peterson	$q_e = \frac{K_{RP} C_e}{1+a_{RP} C_e^{\beta_S}}$	(22)	(Bergmann and Machado, 2015)
Toth	$q_e = \frac{q_{maks} K_T C_e}{[1+(K_T C_e)^{1/nT}]^{nT}}$	(23)	(Bergmann and Machado, 2015)
Liu	$q_e = \frac{q_{maks} (K_g C_e)^{nL}}{1+(K_g C_e)^{nL}}$	(24)	(Bergmann and Machado, 2015)
Khan	$q_e = \frac{q_s b_k C_e}{(1+b_k C_e)^{aK}}$	(25)	(Bergmann and Machado, 2015)

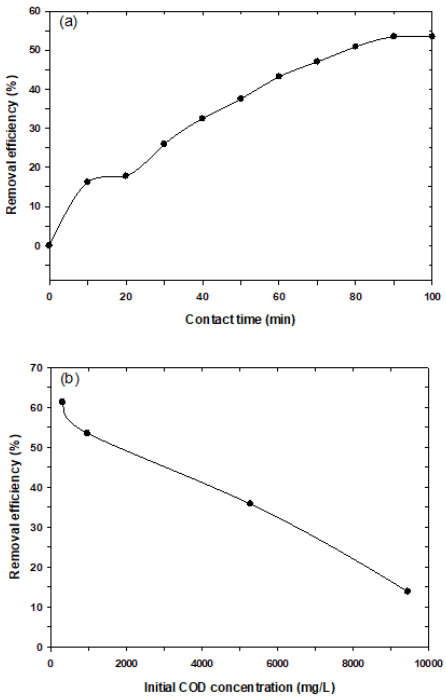

Figure 1. Effect of The Contact Time (A) and Effect of Initial Concentration (B) on The Removal Efficiency

percentage of COD decreased with the increase in initial COD concentration onto polystyrene resin RS 50B (Zhao et al., 2013). Sivarajasekar and Baskar, 2014 observed that the percentage of dye removal decreased with an increase in initial concentration on Gossypium hirsutum adsorbent (Sivarajasekar and Baskar, 2014).

3.3 Kinetic and Equilibrium Studies

The linearization method of kinetic and equilibrium models is the most common method for determining adsorption parameters. However, the linearization of a kinetic and adsorption model may bias the result, and error distribution gets changed (de la Luz-Asunción et al., 2019). Many studies about the application of the non-linear model in the adsorption process have been conducted by researchers currently. Kumar et al., 2008 found that linearization was not a suitable method for predicting the optimum isotherm model (Kumar et al., 2008). The fitting experimental kinetic data was performed using nine kinetic models (pseudo-first-order, pseudo-second-order, intraparticle diffusion, fractional power, Bagham, Elovich, and mixed 1,2 order. Table 2 presents the isotherm models used for fitting experimental data are Langmuir, Freundlich, Dubinin-Radushkevich, Sips, Redlich-Peterson, Toth, Liu and Khan.

Table 3 presents the calculation of five error functions with various kinetic models. It is shown that the SSE error function produced the lowest SNE for five kinetic models (pseudo-first-order, pseudo-second-order, Power, Elovich, and mixed 1.2 order) out of the nine kinetic models. It is followed by the SAE error function for three kinetic models (Bangham, Intraparticle diffusion, and Avrami) and the Hybrid error function for modified pseudo-second-order. The optimum parameter sets are calculated based on minimum SNE value and their value of the coefficient of determination (R^2) and the chi-square (X^2). The

Table 3. The Error Function and SNE for Kinetic Models

	SSE	HYBRID	ARE	MPSD	SAE
Pseudo-first-order					
q_e	6.418	6.25	7.12	5.948	7.016
k_{p1}	0.017	0.018	0.014	0.02	0.015
SSE	0.385	0.391	0.459	0.443	0.441
HYBRID	2.76	2.735	3.198	2.822	3.116
ARE	6.075	6.378	5.207	7.019	5.204
MPSD	12.99	12.798	13.9	12.687	13.83
SAE	1.352	1.439	1.115	1.67	1.101
SNE	4.305	4.395	4.41	4.757	4.325
Pseudo-second-order					
q_e	9.498	9.211	11.33	8.641	10.76
k_{p2}	0.001	0.001	0.001	0.002	0.001
SSE	0.37	0.374	0.49	0.422	0.425
HYBRID	2.523	2.507	3.148	2.586	2.869
ARE	6.308	6.535	5.429	6.967	5.433
MPSD	12.29	12.119	13.65	12.021	13.19
SAE	1.465	1.539	1.241	1.701	1.206
SNE	4.221	4.292	4.509	4.565	4.231
Intraparticle diffusion					
K_{ip}	0.522	0.51	0.513	0.493	0.517
θ	0.001	0.001	0.001	0.002	0.001
SSE	0.702	0.778	0.743	1.175	0.716
HYBRID	3.958	3.721	3.733	4.262	3.796
ARE	7.931	7.681	7.603	8.394	7.659
MPSD	14.1	13.129	13.32	12.518	13.64
SAE	2.107	2.261	2.163	2.896	2.097
SNE	4.199	4.159	4.104	4.885	4.101
Fractional power					
Kp	0.335	0.321	1.208	0.322	0.517
vo	0.606	0.616	0.259	0.614	0.001
SSE	0.341	0.344	7.234	0.353	115.6
HYBRID	1.714	1.694	24.838	1.708	338.8
ARE	5.644	5.743	22.521	5.938	83.03
MPSD	9.201	9.112	29.7	9.094	93.3
SAE	1.521	1.567	7.496	1.659	31.372
SNE	0.223	0.225	0.965	0.23	5
Bangham					
kb	0.298	0.321	0.86	0.322	0.345
m	1.578	1.623	2.738	1.628	1.662
SSE	0.363	0.344	2.754	0.353	0.354
HYBRID	1.738	1.694	11.91	1.708	1.81
ARE	5.695	5.743	15.837	5.938	5.53
MPSD	9.206	9.112	22.96	9.094	9.479
SAE	1.543	1.567	4.705	1.659	1.433
SNE	1.365	1.359	5	1.394	1.347
Elovich					
α	0.301	0.318	0.239	0.334	0.24
β	0.552	0.596	0.467	0.66	0.461
SSE	1.062	1.173	1.933	1.772	1.948
HYBRID	6.515	6.08	14.57	6.898	14.939
ARE	11.289	11.686	10.672	12.232	10.729

	SSE	HYBRID	ARE	MPSD	SAE
MPSD	18.84	17.359	30.25	16.672	30.643
SAE	2.703	3.138	2.244	3.784	2.213
SNE	3.234	3.36	4.42	3.915	4.462
Mixed 1.2 order					
q_e	9.094	8.902	10.788	8.387	10.093
k	0.001	0.001	0	0.001	0.001
f0	0.913	0.932	0.967	0.94	0.876
SSE	0.37	0.374	0.447	0.422	0.427
HYBRID	2.885	2.866	3.433	2.956	3.294
ARE	6.308	6.535	5.403	6.967	5.428
MPSD	13.086	12.958	14.345	12.852	14.059
SAE	1.464	1.538	1.217	1.701	1.206
SNE	4.345	4.417	4.491	4.7	4.383
Modified pseudo-second-order					
q_e	13.338	16.878	26.595	9.28	10.707
k_{fso}	0.001	0.001	0	0.004	0.001
α	0.832	0.761	0.745	0.614	0.949
SSE	0.32	0.32	0.379	0.353	0.379
HYBRID	2.246	2.104	2.237	1.952	2.773
ARE	6.031	5.94	5.432	5.938	6.127
MPSD	11.214	10.636	10.789	9.722	12.626
SAE	1.481	1.514	1.363	1.659	1.378
SNE	4.419	4.328	4.369	4.373	4.831
Avrami					
q_e	9.126	46.703	38.107	49.553	19.89
k_{av}	0.009	0	0.001	0	0.002
n_{av}	0.792	0.639	0.66	0.635	0.683
SSE	0.309	0.335	0.358	0.344	0.331
HYBRID	2.161	1.94	2.026	1.955	2.009
ARE	5.928	5.735	5.461	5.912	5.484
MPSD	10.981	9.848	10.06	9.822	10.187
SAE	1.453	1.545	1.417	1.631	1.377
SNE	4.755	4.648	4.644	4.757	4.554

Table 4. The Value of The Coefficient of Determination (R^2) and Chi-Squared (X^2) Kinetic Models

Model	R^2	X^2
Pseudo-first-order	0.98	0.221
Pseudo-second-order	0.98	0.202
intraparticle diffusion	0.96	0.304
Fractional power	0.98	0.137
Bangham	0.98	0.145
Elovich	0.94	0.521
Mixed 1.2 order	0.98	0.202
Modified pseudo-second-order	0.98	0.147
Avrami	0.98	0.141

result of the coefficient of determination (R^2) and the chi-square are presented in Table 4. The fractional power kinetic model provided a better fit experimental data with the highest R^2 and lowest X^2. However, Bangham, modified pseudo-second-order, and Avrami also fitted well to experimental kinetic data. It can be seen from their R^2 (0.98) and the X^2 (0.145. 0.147 and 0.141).

Non-linear SNE procedure was used to evalu ate eight isotherm models. The calculations of the error function are presented in Table 5. The MPSD error function given the minimum SNE value for Langmuir. Sips. Redlich-Peterson and Liu. The error function produced a minimum SNE value for Freundlich. Toth and Khan models. The Dubinin-Radushke vich had a minimum value of SNE in the SSE error function.

The result of the coefficient determination (R^2) and Chi-squared (X^2) calculation of isotherm models shows in Table 6 that the Khan model fitted well with experimental data (R^2: 0.99961, X^2: 0.03729) and Langmuir (R^2: 0.99478, X^2:0.24902). Langmuir isotherm indicates the forming of adsorbate mono-

Table 5. The Error Function and SNE for Isotherm Models

	SSE	HYBRID	ARE	MPSD	SAE
Langmuir					
q_{maks}	14.858	14.907	14.369	14.894	14.405
K_L	0.00124	0.001211	0.00127	0.00121	0.00123
SSE	0.49	0.498	0.813	0.5	0.863
HYBRID	2.058	1.965	3.168	1.967	3.392
ARE	2.997	2.434	2.012	2.44	2.496
MPSD	4.443	4.011	4.99	4.006	5.342
SAE	1.146	1.079	0.956	1.074	0.999
SNE	4.0066	3.6613	4.3149	3.661	4.7043
Freundlich					
K_f	0.56	0.335	0.208	0.236	0.234
n	2.779	2.385	2.165	2.167	2.237
SSE	6.353	7.591	13.819	9.617	13.896
HYBRID	58.868	41.164	69.746	47.037	68.493
ARE	22.706	18.688	14.935	16.864	15.345
MPSD	47.533	28.436	29.219	24.524	28.633
SAE	4.396	4.997	5.211	5.48	5.043
SNE	4.103	3.47	4.218	3.625	4.18
Dubinin-Radushkevich					
q_e	13.096	13.096	13.064	13.094	13.065
k_{ad}	0.0307	0.0306	0.0306	0.0307	0.0306
SSE	3.613	3.613	3.615	3.613	3.615
HYBRID	95.01	95.01	95.018	95.01	95.017
ARE	25.163	25.159	25.159	25.164	25.159
MPSD	70.71	70.71	70.711	70.71	70.711
SAE	1.984	1.983	1.984	1.984	1.984
SNE	4.99925	4.99868	4.99958	4.99938	4.99956
Sips					
q_{maks}	0.01847	0.018045	0.02081	0.01822	0.01801
βS	1	1	0.9729	0.99767	0.99469
K_R	0.00124	0.001211	0.00143	0.00122	0.00119
SSE	0.49	0.498	0.958	0.506	0.561
HYBRID	4.116	3.93	7.441	3.967	4.426
ARE	2.997	2.434	2.15	2.407	2.682
MPSD	6.284	5.673	7.62	5.664	6.316
SAE	1.146	1.079	1.02	1.075	1.104
SNE	3.89	3.547	4.608	3.546	3.868
Redlich-Peterson					
K_{RP}	0.01847	0.018046	0.01801	0.01801	0.01826
a_{RP}	0.00124	0.00121	0.00125	0.00121	0.00139
g	1	1	1	1	0.98979
SSE	0.49	0.498	0.836	0.5	0.946
HYBRID	4.116	3.93	6.507	3.934	7.342
ARE	2.996	2.434	2.118	2.44	2.018
MPSD	6.282	5.673	7.181	5.666	7.559
SAE	1.146	1.079	0.949	1.074	0.983
SNE	3.91	3.567	4.255	3.566	4.532
Toth					
q_{maks}	13.3964	14.13311	14.4187	14.7564	13.1458
K_T	0.0001	0.0011	0.0013	0.0012	0.0009
n_T	0.5684	0.8245	1.0076	0.9748	0.42117

	SSE	HYBRID	ARE	MPSD	SAE
SSE	0.15	0.281	0.861	0.462	0.207
HYBRID	5.975	2.99	6.697	3.699	10.896
ARE	5.325	3.512	2.092	2.55	6.001
MPSD	17.113	7.407	7.287	5.631	23.947
SAE	0.695	0.962	0.95	1.058	0.458
SNE	2.981	2.405	3.165	2.536	3.674
Liu					
q_{maks}	14.1052	14.62771	14.6306	14.9137	19.4351
K_g	0.00147	0.001299	0.0012	0.0012	0.00041
n_L	1.176	1.044	0.981	0.9977	0.6015
SSE	0.328	0.417	0.757	0.506	3.746
HYBRID	6.413	3.637	5.866	3.967	60.195
ARE	5.856	3.221	1.913	2.407	14.35
MPSD	15.398	6.496	6.743	5.664	45.897
SAE	1.125	1.085	0.983	1.075	2.58
SNE	1.374	0.958	0.961	0.909	5
Khan					
q_s	23.9643	22.3968	35.2548	18.7205	39.2017
b_k	0.00067	0.000742	0.00043	0.00093	0.00037
a_k	1.23315	1.19447	1.49089	1.10241	1.58078
SSE	0.025	0.037	0.599	0.157	0.898
HYBRID	1.143	0.926	6.675	1.581	9.864
ARE	2.236	2.196	4.567	2.245	5.118
MPSD	7.555	5.829	12.504	4.671	15.138
SAE	0.235	0.367	1.029	0.688	1.168
SNE	1.28	1.263	3.942	1.671	5

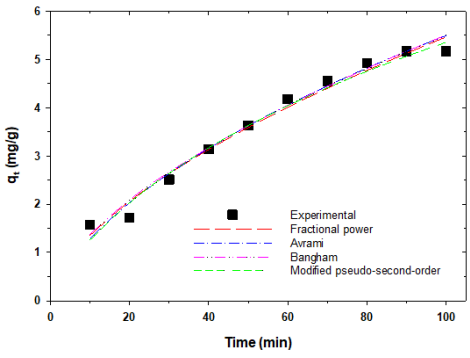

Figure 2. The Best Fitted Non-Linear Kinetic Models

Table 6. The Value of The Coefficient of Determination (R^2) and Chi-Squared (X^2) Isotherm Models

Model	R^2	X^2
Langmuir	0.99478	0.24902
Freundlich	0.92609	3.79572
Dubinin-Radushkevich	0.96367	1.80667
Redlich-Peterson	0.99476	0.50013
Sips	0.9947	0.5059
Toth	0.92611	7.58977
Liu	0.9947	0.50591
Khan	0.99961	0.03729

layer in tapioca liquid waste adsorption (Bergmann and Machado, 2015).

4. CONCLUSIONS

The percentage of COD removal was decreased from 61.29% to 13.66%, with increasing COD concentration from 310 mg/L to 9450 mg/L. Experiment data from adsorption tapioca liquid waste onto modified natural zeolite was analyzed with non-linear regression. Six error function was used to evaluate parameter sets of kinetic and isotherm models according to the minimum of SNE

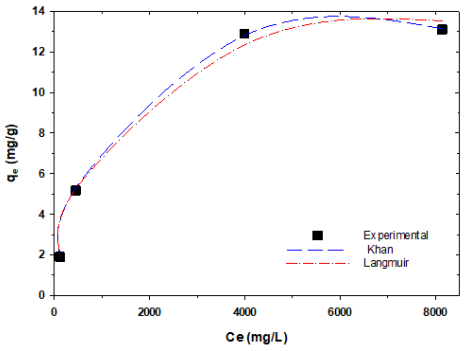

Figure 3. The Best Fitted Non-Linear Isotherm Models

value. The parameter sets were validated with the coefficient of determination (R^2) and Chi-square (X^2). The adsorption of tapioca liquid was well described with fractional power (R^2: 0.98, X^2: 0.137), Avrami (R^2: 0.98, X^2: 0.141), Bangham (R^2: 0.98, X^2: 0.145) and modified pseudo-second-order (R^2: 0.98, X^2: 0.147). The isotherm model was best fitted with the Khan model (R^2: 0.99961, X^2: 0.03729) and Langmuir (R^2: 0.99478, X^2:0.24902).

5. ACKNOWLEDGEMENT

The authors thank the financial support from Institut Teknologi Sumatera (ITERA) for a research grant with the scheme of Penelitian Dasar Hibah Mandiri No. 236/IT9.A/SK/PP/2018.

REFERENCES

Anas, N. A. A., Y. W. Fen, N. A. Yusof, N. A. S. Omar, N. S. M. Ramdzan, and W. M. E. M. M. Daniyal (2020). Investigating the Properties of Cetyltrimethylammonium Bromide/Hydroxylated Graphene Quantum Dots Thin Film for Potential Optical Detection of Heavy Metal Ions. *Materials*, **13**(11); 2591

Bergmann, C. P. and F. M. Machado, editors (2015). *Carbon Nanomaterials as Adsorbents for Environmental and Biological Applications. New York:*. Springer International Publishing

Dada, A. (2012). Langmuir, Freundlich, Temkin and Dubinin-Radushkevich Isotherms Studies of Equilibrium Sorption of Zn 2+ Unto Phosphoric Acid Modified Rice Husk. *IOSR Journal of Applied Chemistry*, **3**(1); 38–45

Darmansyah, S. B. Ginting, D. A. Iryani, R. P. Sari, and D. Supriyadi (2021). Characterization of Modified Lampung Natural Zeolite with Cetyl Trimethyl Ammonium Bromide (CTAB) for Adsorption Industrial Tapioca Wastewater. In *Proceedings of the International Conference on Sustainable Biomass (ICSB 2019)*. Atlantis Press

Darmansyah, D., H. Saputra, S. Ginting, and L. Ardiana (2016). Synthesis and Characterization of Mcm-41 from Coal Fly Ash for Tapioca Wastewater Treatment. *ARPN Journal of Engineering and Applied Sciences*, **11**(7); 4772–4777

de la Luz-Asunción, M., E. E. Pérez-Ramírez, A. L. Martínez-Hernández, V. M. Castano, V. Sánchez-Mendieta, and C. Velasco-Santos (2019). Non-Linear Modeling of Kinetic and Equilibrium Data for The Adsorption of Hexavalent Chromium by Carbon Nanomaterials: Dimension and Functionalization. *Chinese Journal of Chemical Engineering*, **27**(4); 912–919

Edama, N. A., A. Sulaiman, and S. N. A. Rahim (2014). Enzymatic Saccharification of Tapioca Processing Wastes Into Biosugars Through Immobilization Technology (Mini Review). *Biofuel Research Journal*, **1**(1); 2–6

Fito, J., N. Tefera, and S. W. V. Hulle (2017). Adsorption of Distillery Spent Wash on Activated Bagasse Fly Ash: Kinetics and Thermodynamics. *Journal of Environmental Chemical Engineering*, **5**(6); 5381–5388

Guo, J., S. Chen, L. Liu, B. Li, P. Yang, L. Zhang, and Y. Feng (2012). Adsorption of Dye From Wastewater Using Chitosan CTAB Modified Bentonites. *Journal of Colloid and Interface Science*, **382**(1); 61–66

Haerifar, M. and S. Azizian (2014). Fractal-Like Kinetics for Adsorption on Heterogeneous Solid Surfaces. *The Journal of Physical Chemistry C*, **118**(2); 1129–1134

Halim, A. A., H. A. Aziz, M. A. M. Johari, and K. S. Ariffin (2010). Comparison Study of Ammonia and COD Adsorption on Zeolite, Activated Carbon and Composite Materials in Landfill Leachate Treatment. *Desalination*, **262**(1-3); 31–35

Hermiati, E., D. Mangunwidjaja, T. C. Sunarti, O. Suparno, and B. Prasetya (2012). Potential Utilization of Cassava Pulp for Ethanol Production in Indonesia. *Scientific Research and Essays*, **7**(2); 100–106

Ho, Y. and G. McKay (1998). A Comparison of Chemisorption Kinetic Models Applied to Pollutant Removal on Various Sorbents. *Process Safety and Environmental Protection*, **76**(4); 332–340

Khambhaty, Y., K. Mody, S. Basha, and B. Jha (2009). Kinetics, Equilibrium and Thermodynamic Studies on Biosorption of Hexavalent Chromium by Dead Fungal Biomass of Marine Aspergillus Niger. *Chemical Engineering Journal*, **145**(3); 489–495

Kumar, K. V., K. Porkodi, and F. Rocha (2008). Comparison of Various Error Functions in Predicting The Optimum Isotherm by Linear and Non-Linear Regression analysis for The Sorption of Basic Red 9 by Activated Carbon. *Journal of Hazardous Materials*, **150**(1); 158–165

Kuo, C.-Y. (2009). Comparison With As-Grown and Microwave Modified Carbon Nanotubes to Removal Aqueous Bisphenol A. *Desalination*, **249**(3); 976–982

Liu, J., X. Cheng, Y. Zhang, X. Wang, Q. Zou, and L. Fu (2017). Zeolite Modification for Adsorptive Removal of Nitrite from Aqueous Solutions. *Microporous and Mesoporous Materials*, **252**; 179–187

Marczewski, A. (2010). Application of Mixed Order Rate Equations to Adsorption of Methylene Blue on Mesoporous Carbons. *Applied Surface Science*, **256**(17); 5145–5152

Mohadi, R., , Z. Hanafiah, H. Hermansyah, and H. Zulkifli (2017). Adsorption of Procion Red And Congo Red Dyes using Microalgae Spirulina Sp. *Science and Technology Indonesia*, **2**(4); 102–104

Moussout, H., H. Ahlafi, M. Aazza, and H. Maghat (2018). Critical of Linear and Nonlinear Equations of Pseudo-First Order and Pseudo-Second Order Kinetic Models. *Karbala International Journal of Modern Science*, **4**(2); 244–254

Nagy, B., C. Mânzatu, A. Măicăneanu, C. Indolean, L. Barbu-Tudoran, and C. Majdik (2017). Linear and Nonlinear Regression Analysis for Heavy Metals Removal using Agaricus Bisporus Macrofungus. *Arabian Journal of Chemistry*, **10**; S3569–S3579

Netzahuatl-Muñoz, A. R., M. del Carmen Cristiani-Urbina, and E. Cristiani-Urbina (2015). Chromium Biosorption from Cr(VI) Aqueous Solutions by Cupressus lusitanica Bark: Kinetics, Equilibrium and Thermodynamic Studies. *PLOS ONE*, **10**(9); e0137086

Rodríguez, A., J. García, G. Ovejero, and M. Mestanza (2009). Adsorption of Anionic and Cationic Dyes on Activated Carbon from Aqueous Solutions: Equilibrium and Kinetics. *Journal of Hazardous Materials*, **172**(3); 1311–1320

Shen, L., W. Wang, T. Li, Y. Cui, B. Wang, G. Yu, X. Wang, D. Wei, J. Xiao, and S. Deng (2019). Powdered Activated Coke for COD Removal in The Advanced Treatment of Mixed Chemical Wastewaters and Regeneration by Fenton Oxidation. *Chemical Engineering Journal*, **371**; 631–638

Siregar, P. M. S. B. N., N. R. Palapa, A. Wijaya, E. S. Fitri, and A. Lesbani (2021). Structural Stability of Ni/Al Layered Double Hydroxide Supported on Graphite and Biochar Toward Adsorption of Congo Red. *Science and Technology Indonesia*, **6**(2); 85–95

Sivarajasekar, N. and R. Baskar (2014). Adsorption of Basic Red 9 on Activated Waste Gossypium Hirsutum Seeds: Process Modeling, Analysis and Optimization using Statistical Design. *Journal of Industrial and Engineering Chemistry*, **20**(5); 2699–2709

Taffarel, S. R. and J. Rubio (2010). Adsorption of Sodium Dodecyl Benzene Sulfonate from Aqueous Solution using A Modified Natural Zeolite with CTAB. *Minerals Engineering*, **23**(10); 771–779

Verma, S., B. Prasad, and I. M. Mishra (2014). Adsorption Kinetics and Thermodynamics of COD Removal of Acid Pre-treated Petrochemical Wastewater by using Granular Activated Carbon. *Separation Science and Technology*, **49**(7); 1067–1075

Wang, L. C., X. jiong Ni, Y. H. Cao, and G. qun Cao (2018). Adsorption Behavior of Bisphenol A on CTAB-Modified Graphite. *Applied Surface Science*, **428**; 165–170

Wang, S. and Y. Peng (2010). Natural Zeolites As Effective Adsorbents in Water and Wastewater Treatment. *Chemical Engineering Journal*, **156**(1); 11–24

Zhao, Q., Y. Gao, and Z. Ye (2013). Reduction of COD in TNT Red Water Through Adsorption on Macroporous Polystyrene Resin RS 50B. *Vacuum*, **95**; 71–75

